Aust. J. Phys., 1996, **49**, 953–66

Guided Propagation of the Alfvén Wave in a Tokamak

G. G. Borg

Wills Plasma Physics Department, University of Sydney,
Sydney, NSW 2006, Australia.
Present address: Plasma Research Laboratory,
Research School of Physical Sciences and Engineering,
Australian National University,
Canberra, ACT 0200, Australia.

Abstract

Experimental observations are presented of the magnetically guided Alfvén wave excited directly by a small dipole loop antenna located in the scrape-off layer of a tokamak plasma. This wave is excited most efficiently by antenna current elements aligned along the magnetic field and measurements indicate that, at all frequencies below the ion cyclotron frequency, the wave propagates for several transits around the machine with a high degree of localisation about magnetic field lines intersecting the antenna. Along the field, the wave has both a slowly varying amplitude and phase with predominantly radial electric and azimuthal magnetic field components. These experiments demonstrate that the Alfvén wave can propagate as a magnetically guided TEM mode in plasmas which are highly inhomogeneous. We also present a simplified mathematical description of the wave.

1. Introduction

There has been a renewal of interest in direct antenna excitation of the shear Alfvén wave in a laboratory plasma (Gekelman *et al.* 1994, 1995). Important novel applications of this wave have also recently been proposed. Examples are improved helium removal performance of a pump limiter (Shoji *et al.* 1994) and ion mass sensitive RF pumping to remove helium ash from the scrape-off layer of a fusion plasma (Ono 1993; Shoji *et al.* 1994). Experiments on plasma formation by direct excitation of the shear Alfvén wave as a primary ionisation process have also been successfully performed in a stellarator (Lysojvan *et al.* 1995).

In a homogeneous plasma, the shear or torsional Alfvén wave is an ideal magnetohydrodynamic (MHD) mode which propagates at frequencies below the ion cyclotron frequency. This simplified description of the mode predicts that nearly all the wave energy is transported along field lines and no energy across field lines. When excited by an antenna, the Alfvén wave is predicted to propagate as a highly localised disturbance along the magnetic field and does not cross field lines further than the transverse extent of the antenna. In this model, it is assumed that electrons flow along field lines and short out the parallel electric field of the wave. In cool, low-density plasmas where the Alfvén speed is greater than the electron thermal speed, the physical properties of the shear Alfvén wave are altered by electron acceleration along field lines. A CW disturbance excited

0004-9506/96/050953$05.00

by an antenna which is localised in the direction perpendicular to the magnetic field, propagates on a resonance cone at a small angle to the magnetic field and as a long wave-train at the local Alfvén phase speed along the magnetic field (Borg *et al.* 1985). In this limit, the wave is also referred to as the surface quasi-electrostatic wave (SQEW, Vaclavik and Appert 1991) or the cold plasma electrostatic ion cyclotron wave (Ono 1979).

Magnetically guided propagation of the shear Alfvén wave is a well known experimental phenomenon. For example, the geomagnetic micropulsations, which are low-frequency fluctuations in the Earth's magnetic field, are attributed to eigenmode resonances of the magnetically guided Alfvén wave (Cross 1988). This description is based on the ideal MHD model. An alternative theory based on interference of directly excited disturbances of the SQEW has recently been proposed by Bellan (1995) to explain the micropulsations. This claim is based on the fact that, as a result of the resonance cone, the SQEW cannot form standing waves along field lines as would be predicted for the ideal MHD mode.

It is not widely recognised, however, that the shear Alfvén wave can also be strongly guided in laboratory plasmas in regions of high density gradient and along strongly curved magnetic fields. The main laboratory plasma experiments have been described by Cross (1988) and the references therein. In this paper we provide detailed observations of the guided Alfvén wave in a tokamak plasma. These results confirm the validity of a recent theory (Borg 1994), which has demonstrated for the first time using asymptotic techniques that steep density gradients typical of a laboratory plasma periphery have little effect on the guided Alfvén wave for the perpendicular wave numbers necessary to form a transversely localised disturbance. Analysis was confined to a slab plasma with a density gradient perpendicular to a uniform magnetic field and antenna coupling to the shear Alfvén wave whose parallel electron dynamics is dominated by finite electron mass (SQEW). This analysis was restricted to a fixed wave number component k_z, parallel to the magnetic field. In this case, the SQEW propagates perpendicular to the field with a very short wavelength on the low-density side of the Alfvén resonance layer (ARL, Chen and Hasegawa 1974), $\omega = k_z V_A$, where ω is the wave radian frequency and V_A is the Alfvén speed. Interestingly, it was noted that the Alfvén wave undergoes cutoff near the ARL, where it is reflected back toward the low-density side. This result is expected because, for fixed k_z, the wave vector of the SQEW in the direction of the density gradient goes to zero on the low-density side near the ARL. This result was not previously noticed but has recently been confirmed independently by Bellan (1994). It was also demonstrated that, for the range of perpendicular wave numbers necessary to produce a typical experimentally observed guided Alfvén wave, antenna coupling is more efficient than that to the shear Alfvén wave by resonant mode conversion of the fast magnetosonic wave. Plasma heating by antenna excitation of the fast wave which undergoes mode conversion to the Alfvén wave near the ARL forms the basis of the Alfvén wave heating scheme (Chen and Hasegawa 1974).

In Section 2 we develop a theory of the guided Alfvén wave excited by a single parallel current element in a homogeneous plasma. In Section 3 we present the experimental details, in Section 4 the results of a series of experimental observations, and in Section 5 a summary and implications of the results.

2. Theory

We can obtain a good qualitative picture of the guided Alfvén wave by considering the case of antenna coupling in an infinite homogeneous plasma. The equation describing wave propagation in a plasma is

$$\nabla \times \nabla \times \boldsymbol{E} = \mathrm{i}\omega\mu_0 \boldsymbol{J}_0 + k_0^2 \epsilon . \boldsymbol{E}, \tag{1}$$

where $k_0 = \omega/c$ is the vacuum wave number and J_0 is the antenna current. In the low-frequency limit the dielectric tensor is given by

$$\epsilon = \begin{bmatrix} \epsilon_\perp & 0 & 0 \\ 0 & \epsilon_\perp & 0 \\ 0 & 0 & \epsilon_{||} \end{bmatrix} \tag{2}$$

where

$$\epsilon_\perp = c^2/v_\mathrm{A}^2 ,$$

$$\epsilon_{||} = 1 - \frac{\omega_\mathrm{pe}^2}{\omega^2} \approx -\epsilon_\perp/\gamma^2 ,$$

$$\gamma^2 = \frac{\omega(\omega + \mathrm{i}\nu_\mathrm{ei})}{\omega_\mathrm{ci}\,\omega_\mathrm{ce}} ,$$

$$v_\mathrm{A} = \frac{B}{\sqrt{\mu_0 \rho}} ; \qquad \frac{\omega}{\omega_\mathrm{ci}} \ll 1$$

and where ν_ei is the electron–ion collision frequency and $\omega_\mathrm{ci,ce}$ are respectively the ion and electron cyclotron frequencies. The above expression for $\epsilon_{||}$ is valid provided that $\omega \gg k_z\, v_\mathrm{the}$ where v_the is the electron thermal speed and k_z is the component of the wave vector parallel to the uniform magnetic field. It is this component of the dielectric tensor which describes the electron dynamical effects.

After Fourier transformation, equation (1) becomes

$$\boldsymbol{k} \times \boldsymbol{k} \times \boldsymbol{E}(\boldsymbol{k}, \omega) = -\mathrm{i}\omega\mu_0 \boldsymbol{J}_0 - k_0^2 \epsilon . \boldsymbol{E}(\boldsymbol{k}, \omega) .$$

Solving for the electric fields using the dielectric tensor (2) and the divergence of equation (1), we obtain

$$[k^2 - k_\mathrm{A}^2] E_x(\boldsymbol{k}, \omega) = \mathrm{i}\omega\mu_0 J_\mathrm{ex} + \left(1 + \frac{1}{\gamma^2}\right) k_x\, k_z\, E_z(\boldsymbol{k}, \omega) ,$$

$$[k^2 - k_\mathrm{A}^2] E_y(\boldsymbol{k}, \omega) = \mathrm{i}\omega\mu_0 J_\mathrm{ey} + \left(1 + \frac{1}{\gamma^2}\right) k_y\, k_z\, E_z(\boldsymbol{k}, \omega) ,$$

$$[\gamma^2 k_\perp^2 + k_\mathrm{A}^2 - k_z^2] E_z(\boldsymbol{k}, \omega) = \mathrm{i}\omega\mu_0 \gamma^2 J_{ez}(\boldsymbol{k}, \omega) , \tag{3}$$

where $k_\mathrm{A} = \omega/V_\mathrm{A}$. The dispersion relations for wave modes are given by setting the expressions in the brackets on the left-hand sides of these equations to zero.

We conclude that current elements perpendicular to the magnetic field only excite the fast wave whose dispersion relation is $k^2 = k_A^2$. The Alfvén wave whose dispersion relation is $k_k^2 = k_A^2 + \gamma^2 k_\perp^2$ is only excited by current elements parallel to the field. As previously noted, for densities higher than the value at the ARL for which $k_z = k_A$, the wave becomes evanescent in the perpendicular direction. This phenomenon is not relevant for localised disturbances provided the parallel wave number spectrum includes k_z values which are much higher than k_A.

For simplicity we consider the following antenna current distribution:

$$J_{ez} = \frac{J_{0z}}{\pi d_\perp^2}\,\delta(z)\exp\left(-\frac{x^2+y^2}{d_\perp^2}\right), \tag{4}$$

which represents a short field-aligned current element of Gaussian cross section of halfwidth $d_\perp$. The Fourier transform is

$$J_{ez}(\boldsymbol{k}, \omega) = J_{0z}\exp\left(\frac{-d_\perp^2\, k_\perp^2}{4}\right), \tag{5}$$

where k_z is the wave vector along the magnetic field. Using Faraday's law, equations (3) and the limit where $d_\perp \gg \gamma z$, the following expression for the inverse transform of b_θ is obtained for a field-aligned current element:

$$b_\theta = \frac{\mathrm{i}\,\mu_0\, J_{0z}\, k_A \exp(\mathrm{i}\, k_A\, z)}{4\pi}\int_0^\infty \mathrm{d}k_\perp\, J_1(k_\perp\, r)\exp\left(-\frac{d_\perp^2\, k_\perp^2}{4}\right), \tag{6}$$

where J_1 is a Bessel function. This integral can be evaluated to give (Gradsteyn and Ryzhik 1965)

$$\begin{aligned}
b_\theta &= \frac{\mathrm{i}\,\mu_0\, J_{0z}\, k_A \exp(\mathrm{i}\, k_A\, z)}{4\pi r}\left[1-\exp\left(-\frac{r^2}{d_\perp^2}\right)\right],\\
E_r &= \frac{\mathrm{i}\omega\mu_0\, J_{0z}\exp(\mathrm{i}\, k_A\, z)}{4\pi r}\left[1-\exp\left(-\frac{r^2}{d_\perp^2}\right)\right],\\
E_z &= \frac{\mu_0\, V_A\, \gamma^2 J_{0z}\exp(\mathrm{i}\, k_A\, z)}{2\pi d_\perp^2}\exp\left(-\frac{r^2}{d_\perp^2}\right).
\end{aligned} \tag{7}$$

This is the simplest possible description of direct excitation of the SQEW by field-aligned current elements. The broad antenna approximation eliminates field spreading along the resonance cone and also eliminates the need to consider cross-field diffusion of the wave due to parallel resistivity (Cross 1983; Sy 1984). Equations (7) are the only nonzero electromagnetic field components of the wave provided we ignore the effects of finite frequency with respect to ion cyclotron frequency.

The guided Alfvén wave has a simple form. It propagates as a TEM mode guided by its own field-aligned current (proportional to $E_z \ll E_r$), just like the TEM mode of a coaxial cable. The fact that such cables perfectly guide EM waves regardless of frequency, bends in the cable or imperfections in the

dielectric, provides a very good physical insight into the robust nature of the guided Alfvén mode of a magnetised plasma. The wave magnetic field decreases with decreasing plasma density. At low plasma density, the Alfvén wave therefore becomes electrostatic even though its guided nature is unaffected.

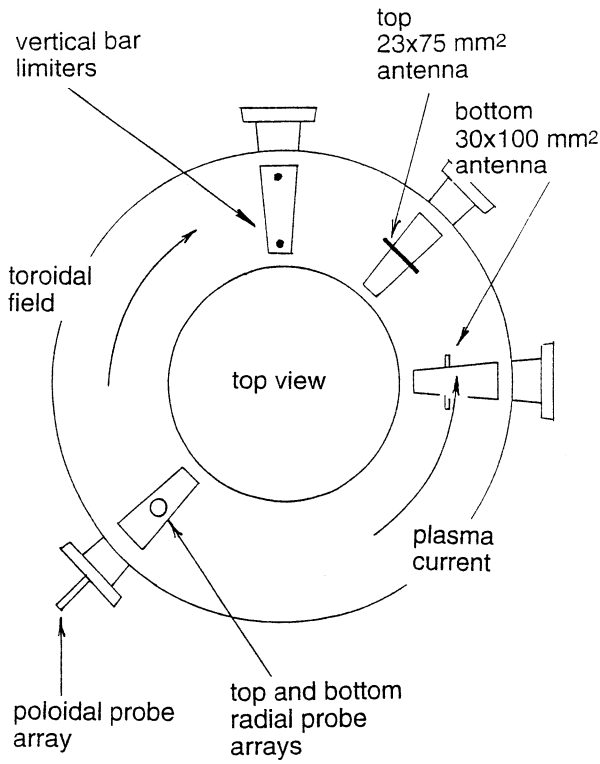

Fig. 1. Experimental arrangement showing the locations of the antennas, the limiters and the poloidal and radial probe arrays.

3. Experimental Arrangement

The experiments were performed in TORTUS (Cross *et al.* 1981), a research tokamak of major radius 0·44 m and minor radius 0·10 m at the University of Sydney. The magnetic field could be varied up to a maximum of 1 T and the plasma current up to 30 kA. The experimental apparatus is shown in Fig. 1.

Waves were excited at low power (a few hundred watts) in the range 1–15 MHz by one of two rectangular dipole loop antennas. The first antenna had dimensions 30 mm×100 mm and was installed below the plasma with its axis in the poloidal direction. The second, of dimensions 23 mm×75 mm, was installed on a radially movable bellows and located above the plasma. This latter antenna was mounted on a rotatable flange so that the effect of antenna orientation with respect to the steady magnetic field lines could be examined.

Experiments were performed using two types of plasma condition. Poloidal profiles of b_θ and b_r in the plasma periphery were performed in a 10–20 kA plasma

of duration 20–30 ms and a magnetic field in the range 0·6–1·0 T. The plasma electron density and temperature were about 10^{19} m^{-3} and 100 eV in the plasma centre and 10^{18} m^{-3} and 20 eV in the plasma periphery. For these conditions, $\omega \gg k_z v_{\text{the}}$ is satisfied and the effects of plasma resistivity are unimportant, so that the SQEW branch of the Alfvén wave is expected to propagate. Radial profiles of the fields were taken in an 8 kA peak plasma of duration 2 ms with toroidal field 0·80 T.

The waves were detected by magnetic probes. In order to detect localised disturbances with the field profiles described by equations (7) of Section 2, high-resolution scans of both the radial and poloidal components of the wave magnetic fields were performed. Two types of magnetic probe were used for this purpose. A poloidal array of six coils, each of approximate length and width 3 mm, were wound on a hollow PVC tube at 20 mm spatial intervals with coil axes parallel to the tube axis. This array could be inserted into an 8 mm OD circular poloidal quartz tube sheath which surrounded the plasma at a minor radius 112 mm, 135° toroidally clockwise (viewed from the top of the machine) from the bottom antenna and 180° toroidally from the top antenna as shown in Fig. 1. The coil axes were therefore aligned in the poloidal direction. A second array of six coils equally spaced over a total length of 100 mm was mounted on a flexible strip of fibreglass with the coil axes normal to the surface. This array could detect the radial component of the wave magnetic field when inserted in the same circular poloidal quartz sheath. Both radial and poloidal components could therefore be measured to confirm the magnetic dipole pattern expected of a TEM-type mode. Both probe arrays could be displaced continuously along the quartz sheath from shot to shot to build up a full poloidal profile and to achieve the 3 mm resolution necessary to discern the highly localised features of the wave. A linear magnetic probe array was also used to measure radial profiles of the fields. This probe was inserted into a radially movable quartz sheath but, because it interfered with the 20 kA discharge, could only be used in the 8 kA plasma current discharge described above.

4. Observations of Guided Wave Propagation at Low Frequency with respect to Ion Cyclotron Frequency

Fig. 2 shows poloidal profiles of the amplitude and phase of b_θ excited by the antenna located on the bottom of the plasma. The antenna was located at minimum minor radius 92 mm with its axis aligned in the poloidal direction. Its 100 mm elements were therefore aligned along the magnetic field for optimum excitation of the guided Alfvén wave. Its 30 mm elements were therefore radially directed. Poloidal profiles were taken at the circular poloidal quartz sheath located 135° from the antenna. For these results the magnetic field was set to 0·59 T and the plasma current to 11 kA. The wave was excited at 4·08 MHz so that $\omega/\omega_{\text{ci}} = 0{\cdot}45 < 1$. In TORTUS, the magnetic field and plasma current are oppositely directed. The direction of positive poloidal angle θ is toward the high-field side (inside the torus) if the antenna is located at $\theta = 0°$.

From Fig. 2 there are three clear peaks observable in the data above a background consisting of an $m = -1$ oscillation of uniform poloidal amplitude. These three peaks are interpreted as a guided Alfvén mode propagating along field lines intersecting the antenna. They cannot be due to Alfvén waves excited

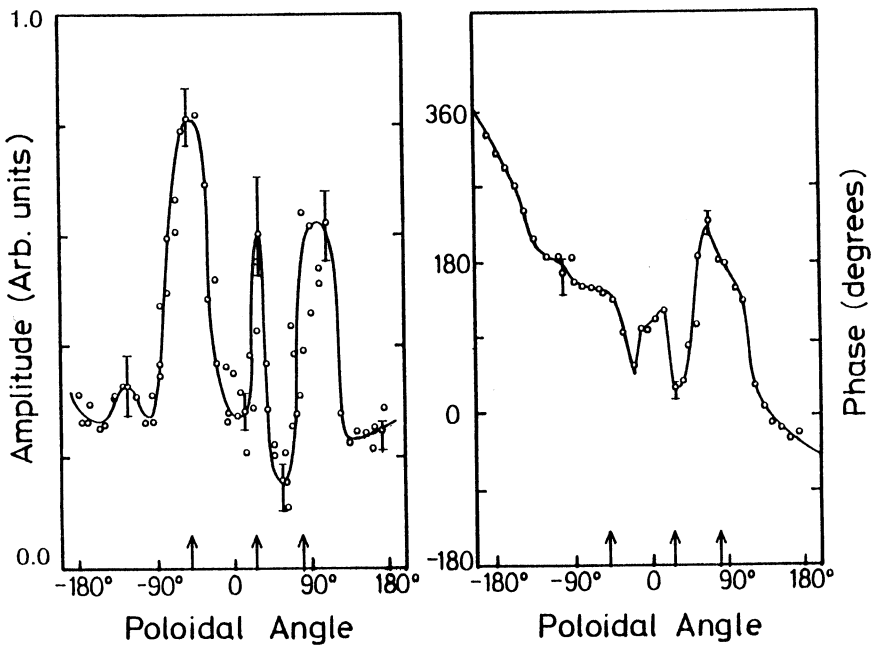

Fig. 2. Poloidal profiles of the amplitude and phase of b_θ taken in the plasma periphery for 4·08 MHz and $B = 0{\cdot}59$ T. The vertical arrows indicate the calculated positions of magnetic field lines passing through the antenna.

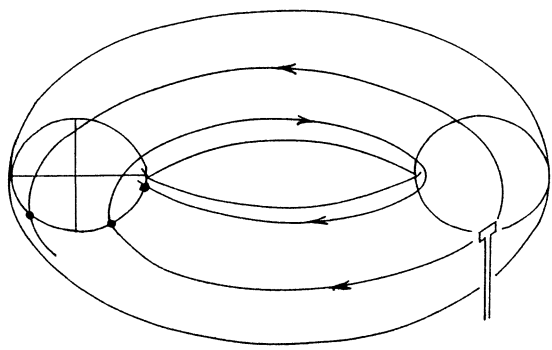

Fig. 3. Schematic illustration of the interpretation of the peaks in Fig. 2.

by mode conversion of the background $m = -1$ surface magnetosonic mode or they would also have a uniform poloidal amplitude (Chen and Hasegawa 1974). There is only one peak for each wave because the poloidal component of the wave field must locally have a single peak. The radial component, as we shall soon see, has to be double-peaked. The interpretation of these peaks is explained schematically in Fig. 3. The peak at $\theta = -50°$ is the wave on its first arrival after propagating 225° counter-clockwise toroidally. The first peak at $\theta = +24°$ is the wave on its first arrival at the probe after travelling 135° clockwise toroidally and the second peak at $\theta = +80°$ is this same wave after one further toroidal transit

of 360° or after travelling 495^0. The calculated positions of the magnetic field line passing through the antenna on the magnetic surface at the toroidal location of the poloidal probe are marked as vertical arrows in Fig. 2. A systematic variation in the positions of peaks with the field line emanating from the antenna and intersecting the probe was confirmed during the rise of the plasma current.

The sharp variation in the amplitude and phase across field lines in the presence of gradients in density, and the possibility of wave reflection due to 'mismatches' and reflections at metallic obstructions along field lines in the plasma periphery, made verification of the wave dispersion difficult without much more detailed three-dimensional measurements. For example, a quartz sheath aligned along a field line yielded phase variations too large and erratic to be compared with the local Alfvén speed in accordance with equations (7). The local dipole character of the fields could however be confirmed. Fig. 4 shows measurements of the poloidal (solid curve as shown in Fig. 2) and the radial component (broken curve) for one wave returning from the clockwise direction on the high-field side and one from the counter-clockwise direction on the low-field side. In the case of the wave on the high-field side, the poloidal component amplitude is low and single peaked and the radial component amplitude high and double-peaked, indicating that the probe intersects the wave near the centre of its dipole pattern. For the wave on the low-field side the poloidal component is large and the radial component is much lower in amplitude but still double-peaked. This suggests that the low-field side wave intersects the probe away from the centre of its dipole pattern.

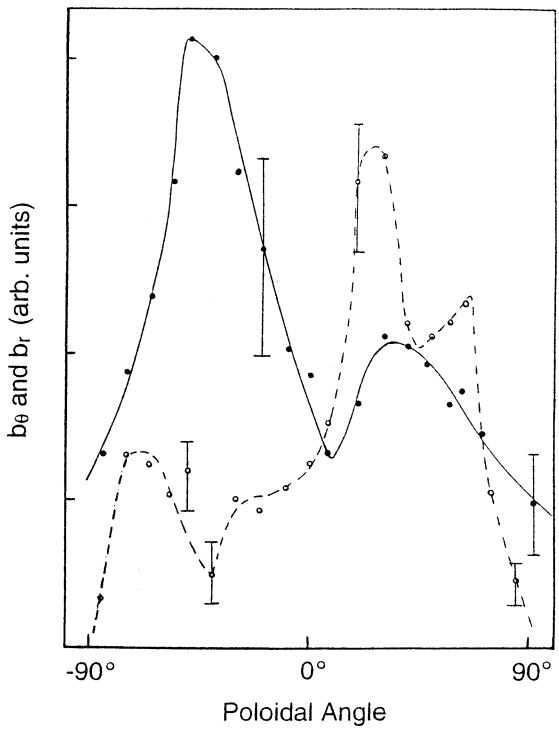

Fig. 4. Poloidal profiles of the poloidal b_θ (solid curve) and radial b_r (broken curve) components, demonstrating the dipole character of the guided Alfvén wave.

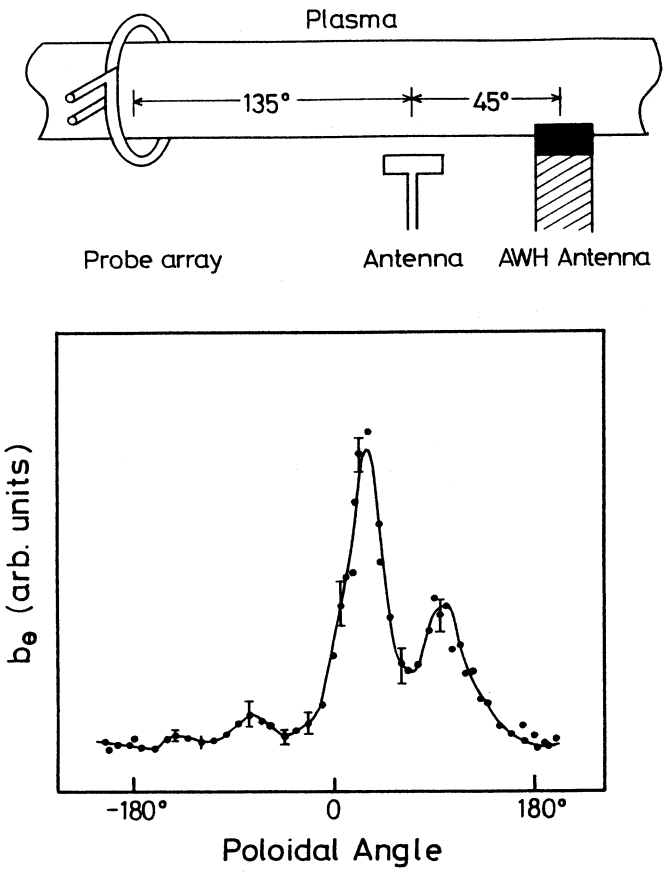

Fig. 5. Experimental arrangement and poloidal profile results, demonstrating the effect of scattering of the guided Alfvén wave by objects in the plasma periphery.

It is fairly clear both theoretically and experimentally that the damping rate of the guided Alfvén mode in TORTUS is very low, yet only a finite number of peaks have been observed. Why is the poloidal profile not a heterogeneous summation of many wave peaks? The most likely hypothesis for the lost peaks is that obstructions in the plasma periphery such as limiters scatter or reflect the wave as they intersect the wave. For example, in these experiments there were two vertical stainless bar limiters installed at $r = 100$ mm, poloidally $\pm 90°$ and toroidally 90° counter-clockwise from the antenna as shown in Fig. 1. Field-line tracing indicates that the high-field side wave travelling clockwise in Fig. 2 and intersecting the probe at $\theta = +24°$ passes the limiter toroidal location at $\theta = +47°$ on its first transit. It subsequently passes the probe at $\theta = +80°$ and the limiter at $\theta = +100°$ on its second transit. At $\theta = +100°$, the wave is very close to the limiter bar on the high-field side so that scattering or reflection can occur. The low-field side wave travelling counter-clockwise intersects the probe at $\theta = -51°$ and the limiter at $\theta = -114°$ on its first transit where it could already be scattered before a second toroidal transit.

This hypothesis was tested by introducing a large obstruction into the plasma boundary close to the antenna but displaced counter-clockwise toroidally as shown in Fig. 5. The obstruction was a shielded Alfvén wave heating poloidal strap antenna covering a 180° poloidal sector on the bottom of the plasma. All direct waves passing in the counter-clockwise direction should be eliminated. The experimental results confirm the hypothesis, as shown in Fig. 5.

Radial profiles of b_θ were taken with the top antenna whose axis could be rotated to verify that the guided Alfvén wave was localised near the plasma periphery. Fig. 6 shows complete vertical radial profiles of b_θ for each orientation of the antenna whose inner poloidal element was located at $r = 101$ mm. The profile of Fig. 6*a* is for the orientation of the antenna axis in the poloidal direction where the 75 mm elements lie along the field for optimal excitation and Fig. 6*b* is for the axis parallel to the magnetic field. These data were taken during a 2 ms, 8 kA plasma. It is clear that the fields are strongly localised toward the plasma periphery where the antenna is located. These profiles were taken through $\theta = 0°$, as shown in Fig. 1, so that they do not coincide with a b_θ peak except when the plasma current is zero. As a result, the signal amplitude decreases as the plasma current rises and increases as it falls, as shown in Fig. 6*a*.

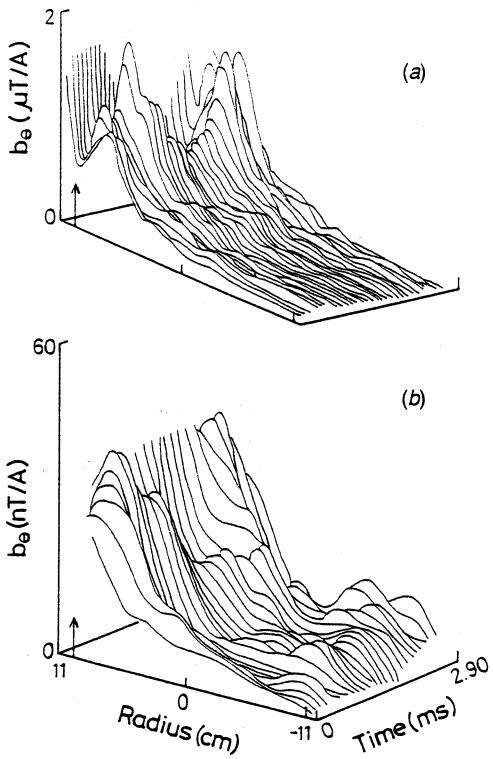

Fig. 6. Radial profiles of b_θ for (*a*) the antenna axis in the poloidal direction and (*b*) the antenna axis parallel to B. The arrow indicates the radial location of the antenna and $r = 0$ is the centre of the plasma.

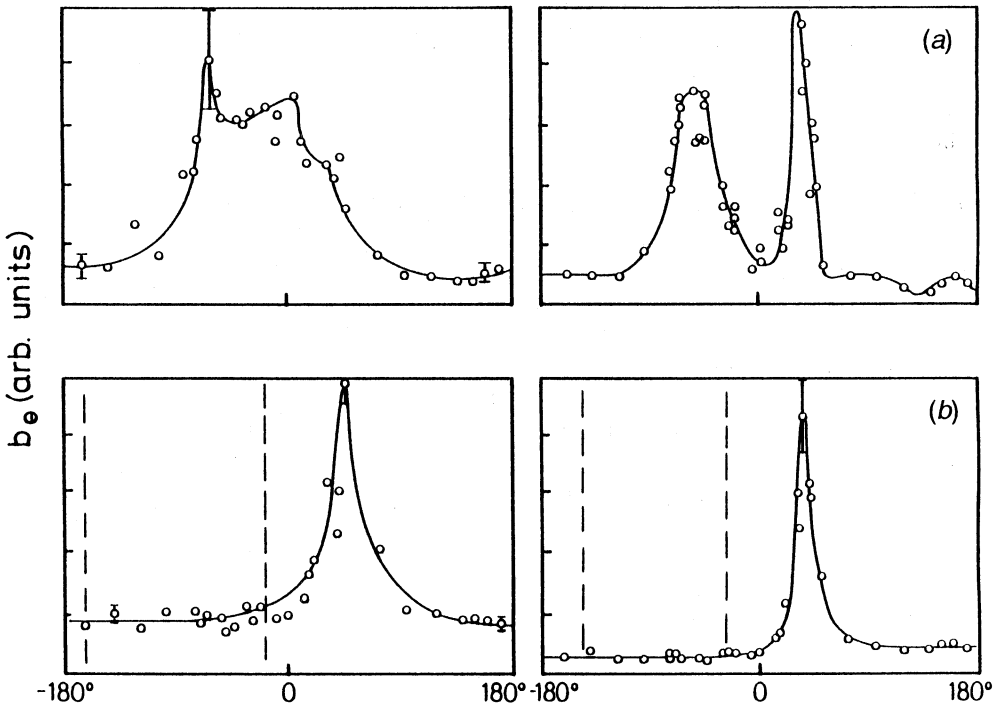

Fig. 7. Poloidal profiles of b_θ taken with the top antenna for (*a*) $\omega/\omega_{ci} = 0{\cdot}65$ and (*b*) $\omega/\omega_{ci} = 0{\cdot}93$ on axis. In the left column are profiles taken with the axis of the antenna aligned parallel to the magnetic field and in the right are profiles with the axis aligned in the poloidal direction.

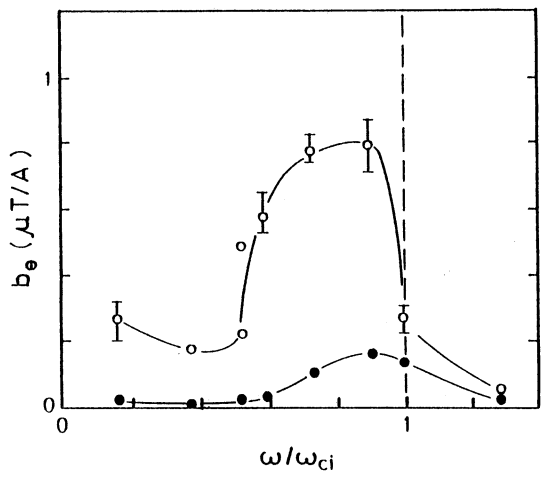

Fig. 8. Dependence of the wave amplitude on the ratio of frequency to ion cyclotron frequency (on axis) for each orientation of the antenna. The open circles are for the antenna axis perpendicular to the magnetic field and the solid circles for the axis parallel to the field.

5. Effects of Finite Frequency with respect to Ion Cyclotron Frequency

Poloidal profiles of b_θ taken with the top antenna are shown in Fig. 7. In Fig. 7*a* the ratio of frequency to ion cyclotron frequency is $\omega/\omega_{ci} = 0{\cdot}65$ on axis and in Fig. 7*b*, $\omega/\omega_{ci} = 0{\cdot}93$ on axis. In the left column are profiles taken with the axis of the antenna aligned parallel to the magnetic field and in the right column profiles with the axis aligned in the poloidal direction, as was the case for Fig. 2. The amplitudes have been normalised to their maximum values. Fig. 7*a* on the right shows only one peak on each side of $\theta = 0°$ which can again be explained by rays travelling on the low- and high-field sides of the antenna being intercepted by the limiter after their first transit. On the left the profile is more spread out, suggesting that the pattern emanates from the whole length of the antenna. This should be compared with the case of a large Alfvén wave heating antenna which shows rays emanating principally from the radial end elements of the antenna (Murphy 1989). In this orientation the antenna can only excite the Alfvén wave at finite frequency (Borg 1987).

In Fig. 7*b* we see that no peak is observed in the region between the dashed lines where the frequency is above the local ion cyclotron frequency. Due to its short perpendicular wavelength, the guided Alfvén wave has negligible evanescent fields in the low-field regions above the ion cyclotron frequency.

Absolute measurements of the dependence of the wave amplitude on the ratio of frequency to ion cyclotron frequency (on axis) are shown in Fig. 8 for each orientation of the antenna. The toroidal field was 0·80 T on axis for these experiments. The measurements were taken at the position of the first peak in Fig. 7 at $\theta > 0°$ with the antenna fixed at an innermost radius 101 mm so as not to disturb the plasma and so that the poloidal probe was located at the midpoint of the two antenna elements. The peak amplitude increases with frequency and decreases rapidly to zero when the ion cyclotron layer crosses the approximate probe position. These observations are expected of the Alfvén wave, which cannot propagate above the ion cyclotron frequency. Just the same, when the frequency is above the ion cyclotron frequency, the Alfvén wave is evanescent and its evanescent length may be long enough for the wave to be detectable at the probe (Ballico and Cross 1990). For the case of Fig. 8, where the frequency is only about 1·3 times the ion cyclotron frequency, the approximate evanescent length of the wave is short compared with the distance from the antenna to the probe.

It is interesting to note that, at low frequency, the b_θ amplitude decreases with increasing frequency. According to equations (7), however, the wave amplitude should increase with increasing frequency. The best explanation for this effect is that the displacement of the resonance cone (Borg *et al.* 1985) located at $r = \gamma z$ has to be taken into account if the antenna and probe occupy fixed locations. At $\omega/\omega_{ci} \approx 0{\cdot}17$ and $z \approx 1{\cdot}4$ m, we have $\gamma z \approx 6$ mm, suggesting that the peak in b_θ may be due to the resonance cone crossing the probe. Because $d_\perp \approx 5$ mm, the theory leading to equations (7) breaks down for $\omega/\omega_{ci} > 0{\cdot}17$.

6. Conclusions

Experimental observations confirm that the Alfvén wave excited by a localised antenna aligned with current elements parallel to the steady magnetic field

propagates as a highly localised TEM mode along field lines intersecting the antenna. The results also demonstrate that the guidance is not affected by finite frequency with respect to ion cyclotron frequency, except when the frequency exceeds the ion cyclotron frequency and the wave ceases to propagate. Antennas with purely perpendicular current elements also excite the guided Alfvén wave but only at finite frequency with respect to ion cyclotron frequency. For non-localised antennas that are spread across field lines, we expect that the guided wave will form a coherent mode along field lines, but an incoherent mode across field lines because wavelets from different regions of the antenna will rapidly lose their phase coherence.

The concentration of energy along field lines is optimal for the production of large electric fields and ponderomotive forces, especially in the vicinity of the ion cyclotron frequency as shown in Fig. 8. According to equations (7), the electric field amplitude E_r is not sensitive to the plasma density, whilst E_z increases as the density is decreased. Hence the Alfvén wave is suitable for plasma formation during the low-density plasma start-up phase in stellarators, as demonstrated by Lysojvan *et al.* (1995).

Acknowledgments

The author would like to thank Assoc. Prof. R. C. Cross for his encouragement. This work was supported by the ARGS, the NERDDC and the Science Foundation for Physics within the University of Sydney. Technical assistance by V. Buriak, P. Dennis and J. Piggott is gratefully acknowledged.

References

Ballico, M. J., and Cross, R. C. (1990). *Fusion Engineering Design* **12**, 197.
Bellan, P. M. (1994). *Phys. Plasmas* **1**, 3523.
Bellan, P. M. (1995). *Bull. Am. Phys.* **40** (11), 8Q34, 1844.
Borg, G. G. (1987). PhD thesis, University of Sydney.
Borg, G. G. (1994). *Plasma Phys. Controlled Fusion* **36**, 1419.
Borg, G. G., Brennan, M. H., Cross, R. C., Giannone, L., and Donnelly, I. J. (1985). *Plasma Phys. Controlled Fusion* **27**, 1125.
Chen, L., and Hasegawa, A. (1974). *Phys. Fluids* **17**, 1399.
Cross, R. C. (1983). *Plasma Phys. Controlled Fusion* **25**, 1377.
Cross, R. C. (1988). 'An Introduction to Alfvén Waves' (Adam Hilger: Bristol).
Cross, R. C., James, B. W., Kirby, H. C., Lehane, J. A., and Simpson, S. W. (1981). *Atomic Energy Aust.* **24**, 2.
Gekelman, W., Leneman, D., Maggs, J., and Vincena, S. (1994). *Phys. Plasmas* **1**, 3775.
Gekelman, W., Vincena, S., and Leneman, D. (1995). *Bull. Am. Phys.* **40** (11), 8Q03, 1839.
Gradsteyn, I. S., and Ryzhik, I. M. (1965). 'Tables of Integrals, Series and Products' (Academic: New York).
Lysojvan, A., Moiseenko, V. E., Plyusnin, V. V., Kasilov, S. V., Bondarenko, V. N., Chechkin, V. V., Fomin, I. P., Grigor'eva, V. G., Konovalov, V. G., Koval'ov, S. V., Litvinov, A. P., Mironov, Yu. K., Nazarov, N. I., Pavlichenko, O. S., Pavlichenko, R. O., Shapoval, A. N., Shibenko, A. I., and Volkov, E. D. (1995). *Fusion Engineering Design* **26**, 185.
Murphy, A. B. (1989). *Plasma Phys. Controlled Fusion* **31**, 21.
Ono, M. (1979). *Phys. Rev. Lett.* **42**, 1267.
Ono, M. (1993). Investigation of electrostatic waves in the ion cyclotron range of frequencies in L-4 and ACT-1. Rep. No. PPPL-2900, Princeton.
Shoji, T., Sakawa, Y., Tsuji, K., Watari, T., and Finken, K. H. (1994). New method to improve He-removal performance of pump limiter by RF ponderomotive force. Rep. No. PSC-37, National Institute for Fusion Science.

Sy, W. N.-C. (1984). *Plasma Phys. Controlled Fusion* **26**, 915.
Vaclavik, J., and Appert, K. (1991). *Nucl. Fusion* **31**, 1945.

Manuscript received 5 January, accepted 29 February 1996